Compression Behavior of Municipal Solid Waste: Immediate Compression

Christopher A. Bareither[1]; Craig H. Benson[2]; and Tuncer B. Edil[3]

Abstract: An evaluation of scale effects, stress, waste segregation, and waste decomposition on the immediate compression behavior of municipal solid waste is presented. Laboratory experiments were conducted in 64-, 100-, and 305-mm-diameter compression cells. A field-scale experiment [Deer Track Bioreactor Experiment (DTBE)] was conducted on waste of the same composition and material properties. A methodology is presented for determining the end-of-immediate compression strain (ε_{EOI}) that is applicable to both laboratory- and field-scale data. The compression ratio (C_c') was comparable between tests conducted in 100- and 305-mm compression cells. Compression tests in 305-mm cells conducted on six wastes (three size-differentiated fresh wastes and three decomposed wastes) yielded C_c' ranging from 0.22 to 0.28 in the stress range of 25–100 kPa. A similar C_c' (0.23) was determined for the DTBE (20–67 kPa). The variation in C_c' is related to the waste compressibility index (WCI), which is a function of waste dry weight water content, dry unit weight, and the percent contribution of biodegradable organic waste (paper/cardboard, food waste, yard waste). A compilation of laboratory data from this study and the literature yielded a predictive relationship for the C_c' and WCI. The C_c' can be estimated within ± 0.087 for a given WCI using this relationship. **DOI: 10.1061/(ASCE)GT.1943-5606.0000672.** © *2012 American Society of Civil Engineers.*

CE Database subject headings: Solid wastes; Municipal wastes; Compression; Settlement; Landfills; Sustainable development.

Author keywords: Solid waste; Compression; Settlement; Landfills; Bioreactors; Sustainability.

Introduction

Municipal solid waste (MSW) settlement is a result of physical and biochemical mechanisms defined by three processes: immediate compression, mechanical creep, and biocompression (Sowers 1973; Bjarngard and Edgers 1990; Edil et al. 1990; Kavazanjian et al. 1999; El-Fadel and Khoury 2000; Marques et al. 2003; Sivakumar Babu et al. 2010; Gourc et al. 2010). The initial rapid accumulation of strain upon stress increase is immediate compression. Strain accumulation continues after immediate compression due to mechanical creep and biocompression (Sowers 1973; Rao et al. 1977; Bjarngard and Edgers 1990; Edil et al. 1990). Mechanical creep is a physical compression process where void volume decreases with time as individual waste constituents yield under stress and slippage occurs at particle contacts. Biocompression involves biochemical processes primarily associated with anaerobic decomposition of the organic fraction.

Immediate compression of MSW has generally been referred to as primary compression in relation to traditional soil mechanics principles. However, modern landfills are designed to remain unsaturated (e.g., Benson et al. 2007; Bareither et al. 2010a), and primary compression in soil corresponds to consolidation of solids as pore water pressure dissipates (Terzaghi et al. 1996). Additionally, the hydraulic conductivity of waste is typically on the same order of magnitude as sand and gravel, which suggests excess pore pressure dissipates rapidly upon loading (El-Fadel and Khoury 2000). Thus, the term immediate is used herein instead of primary to distinguish the initial compression phase in MSW from conventional primary compression in soil.

A common parameter used to predict the immediate compression strain (ε_i) in MSW is the compression ratio (C_c')

$$\varepsilon_i = C_c' \cdot \log \frac{\sigma_{vo}' + \Delta\sigma_v'}{\sigma_{vo}'} \quad (1)$$

where σ_{vo}' = existing vertical effective stress and $\Delta\sigma_v'$ = additional vertical effective stress to induce compression (Holtz and Kovacs 1981; Oweis and Khera 1990). The constrained modulus (e.g., Beaven and Powrie 1995) and coefficient of volume change (e.g., Chen et al. 2010a) have also been used to represent immediate compression. However, these two parameters have been shown to be a function of applied vertical stress, whereas Stoltz et al. (2010) determined a single C_c' for MSW that was applicable for stress ranging from 20 to 300 kPa.

Beaven and Powrie (1995) report similar ranges of C_c' for unprocessed and shredded MSW (maximum particle size < 150 mm) tested in a 2-m-diameter cell. Durmusoglu et al. (2006) report similar C_c' for MSW tested in 64- and 711-mm cells with varying cell diameters to the particle size ratios. In contrast, Hossain and Gabr (2009) indicated that C_c' increased as the ratio of the cell diameter to the maximum particle size increased (i.e., smaller waste particles) for a given size cell owing to reduced reinforcement between the particles. However, Hossain and Gabr (2009) report similar C_c' for 64-, 100-, 200-, and 300-mm-diameter compression cells when

[1]Research Associate, Dept. of Geological Engineering, Univ. of Wisconsin–Madison, Madison, WI 53706 (corresponding author). E-mail: bareither@wisc.edu

[2]Wisconsin Distinguished Professor, Director of Sustainability Research & Education, and Chair, Civil & Environmental Engineering, Dept. of Geological Engineering, Univ. of Wisconsin–Madison, Madison, WI 53706. E-mail: chbenson@wisc.edu

[3]Professor, Dept. of Geological Engineering, Univ. of Wisconsin–Madison, Madison, WI 53706. E-mail: tbedil@wisc.edu

Note. This manuscript was submitted on March 2, 2011; approved on November 22, 2011; published online on December 10, 2011. Discussion period open until February 1, 2013; separate discussions must be submitted for individual papers. This paper is part of the ***Journal of Geotechnical and Geoenvironmental Engineering***, Vol. 138, No. 9, September 1, 2012. ©ASCE, ISSN 1090-0241/2012/9-1047–1062/$25.00.

the ratio of the cell diameter to the maximum particle size was consistent.

Compression ratio has been reported to decrease with decreasing organic fraction (Sowers 1973; Chen et al. 2009) as well as with the increasing contribution of incompressible materials (Kavazanjian et al. 1999; Dixon et al. 2008). An increase in MSW density has also been reported to cause a decrease in C_c' (Landva et al. 2000; Chen et al. 2009). Chen et al. (2009) reported trends of decreasing C_c' with increasing waste depth and increasing waste age (i.e., waste decomposition). Hossain et al. (2003) showed an opposite relationship, where C_c' increased with more decomposed waste (i.e., decreasing organic fraction). Higher C_c' have been reported for waste with higher water contents but having similar composition and dry unit weight (Vilar and Carvalho 2004; Reddy et al. 2009a).

While these past studies have demonstrated the effects of scale, waste processing, and material properties on the immediate compression behavior of MSW, a systematic evaluation of these factors has not been conducted. Additionally, the relevance of past findings to field conditions is not known. These laboratory investigations, as well as others, have not directly compared laboratory- and field-scale compression behavior.

The objectives of this study were to evaluate scale effects, stress, waste segregation, and waste decomposition on C_c' and to evaluate the efficacy of laboratory experiments to represent field-scale compression behavior. To evaluate the scale effects, laboratory compression tests were conducted in 64-, 100-, and 305-mm-diameter compression cells with waste having similar composition, dry unit weight, and water content. Waste segregation effects were investigated by testing three size-differentiated fractions of fresh MSW; waste decomposition effects were investigated by testing waste at three different states of decomposition. Decomposed MSW was created from fresh MSW in laboratory anaerobic reactors. Data from these laboratory experiments are compared with data from a field-scale experiment conducted on fresh MSW with similar composition. Data from this investigation along with data from the literature were used to develop a predictive tool that relates C_c' to waste composition and material properties.

Materials and Methods

Deer Track Bioreactor Experiment

Field-scale compression data were obtained from the Deer Track Bioreactor Experiment (DTBE); a lysimeter experiment to assess the influence of leachate addition on the physical, chemical, and biological behavior of MSW (Bareither et al. 2012). A schematic of the DTBE is shown in Fig. 1. The DTBE consists of a cylindrical (2.4 m diameter by 8.4 m tall) steel drainage lysimeter placed vertically within the waste mass of an operating landfill (Deer Track Park, Watertown, Wisconsin).

Waste excavated from the landfill was placed in a 30-m^3 roll-off box and subsequently (i.e., 1–2 days) used to fill the lysimeter in 0.3-m-thick waste lifts (initial thickness = 6.85 m). The waste was dropped from an excavator bucket into the lysimeter, manually distributed to achieve level surfaces, and compacted to the extent practical using hand tools. The mass of waste in the lysimeter was monitored by periodically weighing the roll-off box during filling with the landfill scale ($\pm$10 kg). The DTBE was instrumented to monitor water content, pore pressure, temperature, and settlement at various depths in the waste column (Fig. 1). Gas generation and gas composition were not monitored. The DTBE was operated for 1,067 days, with leachate dosing initiated on Day 399. The instrumentation, operation, data, and analyses are described in Bareither et al. (2012).

Settlement plates were staggered vertically to evaluate the density and stress effects on waste behavior (Fig. 1). The settlement monitoring system consisted of steel plates (600 mm square, 6.4 mm thick) attached to 19-mm-diameter steel rods extending to the top of the lysimeter. The rods were encased in 50-mm-diameter PVC pipes to decrease frictional resistance with the surrounding materials. Settlement was monitored during construction of the lysimeter using a surveying level and measuring tapes affixed to each settlement rod. Settlement of each plate was recorded following deposition of individual waste lifts to assess immediate compression. The vertical position of the lysimeter was also measured during construction; movement was negligible. After construction, the settlement was monitored via electronic position transducers (SpaceAge Control, Inc., Model 162-3405; Palmdale, California) connected to the settlement rods. The transducers were mounted on a rigid frame attached to the top of the lysimeter, which ensured that vertical displacements were not confounded by the settlement of the lysimeter.

Municipal Solid Waste

Fresh MSW

The MSW for the laboratory experiments was collected during construction of the DTBE. This MSW had been in place for approximately 3–4 months prior to sampling and is considered as fresh (F) MSW. Twelve F-MSW samples ranging between 35 and 76 kg (dry mass) were analyzed for composition. Each sample was initially screened on a 25-mm screen to separate small unidentifiable waste constituents and soil or soil-like materials from larger identifiable waste constituents. Particles retained (R) on the 25-mm screen (F-R25) were separated by hand into material-related categories (e.g., paper, wood, metal). Material passing (P) the 25-mm screen (F-P25) was aggregated into a single waste fraction. All waste materials were air-dried following composition analysis. The composite F-MSW contained approximately equal mass fractions (dry mass basis) of F-P25 (46.6%) and F-R25 (53.4%).

A summary of the waste composition for F-MSW, F-R25, and F-P25 is given in Table 1. The F-P25 composition was assessed on select subsamples from the larger F-P25 fraction, with material passing a No. 4 sieve collectively referred to as soil-like material (Bareither et al. 2010b). The average F-MSW composition (Table 1) is similar to that reported by Hull et al. (2005) for 1–3-year-old MSW. The negligible yard waste component in the fresh waste is a result of a yard waste ban in Wisconsin landfills. The negligible food waste fraction (Table 1) is attributed to decomposition before waste was exhumed for use in the DTBE. The F-P25 composition consisted predominantly of inert material, with approximately 85% characterized as soil-like, gravel/inerts, and glass (Table 1). The F-R25 sample contained greater than 70% bulky waste constituents, such as paper/cardboard, plastic, textiles, and wood. Thus, segregating F-MSW into F-P25 and F-R25 fractions distinctly changes the waste composition.

MSW Processing

Waste constituting F-R25 was shredded in a low-speed high-torque shredder to a maximum particle size of 25 mm. Material groups were shredded individually and then recombined to the average waste composition of F-MSW and F-R25 (Table 1) as needed for experimentation.

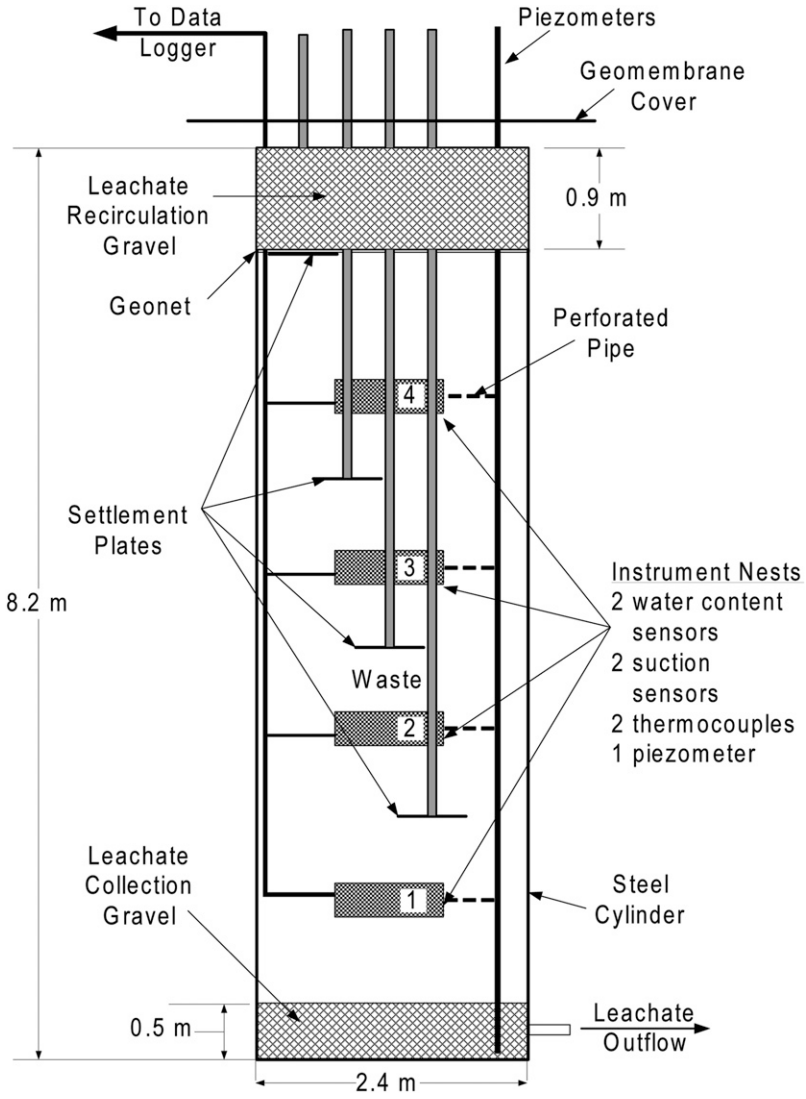

Fig. 1. Schematic of the DTBE lysimeter; initial waste thickness below the settlement plates: Plate 1 = 1.80 m, Plate 2 = 3.80 m, Plate 3 = 5.52 m, and Plate 4 = 6.85

Table 1. Waste Composition for Fresh Wastes (F-MSW, F-P25, and F-R25) Used in This Study

Material	F-MSW	F-R25	F-P25
Paper/cardboard	19.0	32.2	6.1
Flexible plastic	5.2	9.9	0.6
Rigid plastic	5.6	9.1	2.1
Textile	2.9	5.3	0.4
Wood	7.8	13.7	1.6
Gravel/inerts	17.0	14.3	18.2
Yard waste	0.3	0.2	0.4
Food waste	1.1	0.3	1.9
Metal	5.6	9.6	0.7
Glass	2.9	0.9	5.2
Miscellaneous	2.8	4.4	1.1
Soil-like[a]	29.8	0.0	61.8

Note: F-MSW = initial waste composition of the DTBE; F-R25 = initial waste from DTBE retained on a 25-mm screen; and F-P25 = initial waste from DTBE passing a 25-mm screen.

[a]Material passing through a No. 4 sieve (4.75 mm).

MSW Decomposition

Approximately 450 kg of shredded and recombined F-MSW was divided between three 0.27-m^3 laboratory reactors for anaerobic decomposition (Bareither 2010). Waste specimens were prepared to an initial dry unit weight (γ_d) of 6.0 kN/m^3 and dry weight water content (w_d) of 28%, which were similar to the average initial conditions of the DTBE (6.3 kN/m^3, 33%). A small (2 kPa) gravel surcharge was placed on the surface of each waste specimen that was representative of the interim landfill cover.

Waste temperature was maintained between 30 and 40°C using electric heaters affixed to the sides of the reactors. Two 10-L doses of leachate, sampled from the Deer Track Park Landfill (Watertown, Wisconsin), were added to each reactor to inoculate the waste with an active anaerobic microbial community. Effluent leachate from the reactors was recirculated at a rate of 1 L every 2–3 days to accelerate waste decomposition. Methane production was monitored to assess decomposition progression. The reactors were destructively sampled at three progressively higher cumulative methane yields corresponding to three levels of decomposition: low degraded (LD), medium degraded (MD), and high degraded (HD).

MSW Characteristics

The cumulative methane yield from each reactor; cellulose (C), hemicellulose (H), and lignin (L) contents; [(C+H)/L] ratio; volatile solids (VS); and biochemical methane potential (BMP) for the six wastes used in this study are tabulated in Table 2. A description of the methods used to determine the chemical characteristics of the wastes is given in Bareither et al. (2010b). For LD, MD, and HD, the C and H contents, [(C+H)/L] ratio, and BMP decreased, indicating that F-MSW in the reactors decomposed.

The BMP and BMP/VS ratio for LD, MD, and HD both decreased with increasing reactor methane yield (Table 2). This indicates that the level of waste decomposition increases from LD to MD and from MD to HD. The inherent heterogeneity in the chemical properties of the components contained in each biodegradable material group lead to the lack of trends in C, H, [(C+H)/L] ratio, and VS between the three levels of decomposed waste. For example, the paper/cardboard fraction is the primary biodegradable fraction of F-MSW; however, components comprising the paper/cardboard fraction (e.g., office paper, newsprint, corrugated cardboard) have varying rates of decomposition and cumulative methane yield (Owens and Chynoweth 1993; Eleazer et al. 1997; Staley and Barlaz 2009). Thus, while the initial waste composition (F-MSW in Table 1) was consistent between the three 0.27-m^3 laboratory reactors, the chemical signature of the F-MSW constituents may have been variable.

Specific Gravity

The bulk specific gravities (G_s) of F-MSW, LD, MD, and HD were measured using a modified water pycnometer as described in Breitmeyer (2011). The specific gravities of F-MSW, LD, MD, and HD are summarized in Table 2. The specific gravity of the decomposed waste (LD, MD, and HD) is shown as a function of reactor methane yield in Fig. 2. The specific gravity increased with higher levels of decomposition (i.e., higher methane yield), corresponding to the loss of organic materials (e.g., paper) that have high volume and low mass.

Laboratory Compression Experiments

Apparatus

Compression cells were fabricated where stress and temperature could be controlled and leachate and gas could be managed. A schematic of the 305-mm-diameter compression cell is shown in Fig. 3(a) and a schematic of the 64- and 100-mm-diameter compression cells is shown in Fig. 3(b). The cells consisted of aluminum cylinders (9.5-mm wall thickness) with inside diameters of 64, 100, and 305 mm. Cylinders were placed between a 19-mm-thick aluminum top plate and a 25-mm-thick aluminum base plate, which were joined with tie rods. O-rings were used to create gas- and watertight seals between the cylinder and the top and base plates. A hole in the top plate allowed free displacement of a stainless-steel loading rod (a 38-mm-diameter rod for the 305-mm cell and a 19-mm-diameter rod for the smaller cells). A gas-tight Viton membrane provided a seal between the loading rod and the top plate.

Liquid could be added to a test specimen through a liquid injection system in the aluminum load/liquid distribution plate and collected via effluent ports in the base plate. Stainless-steel screens (No. 100 mesh) were placed between the distribution and drain plates and the test specimen to prevent clogging of the liquid distribution and collection systems. Gas generated during testing passed through a gas outlet located in the headspace above the test specimen and was collected in Flexfoil gas bags (SKC, Inc.; Forty Eight, Pennsylvania).

In the 305-mm cells, liquid could be distributed over the specimen surface through the PVC liquid distribution plate [Fig. 3(a)]. Grooves in the load plate and perforations in the PVC liquid distribution plate promoted uniform distribution of liquid on the specimen. Effluent liquid was collected in the base plate after passing through a perforated PVC drain plate.

Stainless-steel drainage plates employing the ball-bearing design presented in Ng et al. (2006) were used in lieu of the perforated PVC plates in the 64- and 100-mm cells [Fig. 3(b)]. The same top plate, base plate, vertical loading system, and tie rods were used for both 64- and 100-mm cells. An interchangeable base plate, stainless-steel ball-bearing drainage plates, load/liquid distribution plate, and aluminum cylinder were fabricated separately to accommodate the 64- and 100-mm-diameter specimens. The interchangeable base plate was bolted in place through the base plate and aligned with the effluent ports.

A 305-mm-diameter pneumatic air cylinder was used to apply force to the loading rod in the 305-mm cells [Fig. 3(a)], which was then distributed to the test specimen. Measurements of the force and displacement were recorded during testing using a personal computer equipped with a National Instruments data acquisition board (PCI-6014) and *LabVIEW* software. A linear variable displacement transducer (LVDT) from Omega Engineering, Inc. (Stamford, Connecticut, LD621-100) was used to measure displacement (100 ± 0.02 mm) and a load cell from Virtual Measurement and Control (Santa Rosa, California, VLC-110) was used to measure force (66.9 ± 0.01 kN). The vertical force applied to the test specimens was maintained by a feedback-controlled pressure regulator (Proportion-Air, McCordsville, Indiana; QB1) connected to the pneumatic air cylinder.

A dead-weight loading system consisting of a rectangular aluminum plate fixed in a horizontal plane by two linear bearings sliding on vertical precision steel rods [Fig. 3(b)] was used to apply

Table 2. Cellulose, Hemicellulose, and Lignin Contents; (Cellulose + Hemicellulose)/Lignin; Volatile Solids; Biochemical Methane Potential; and Specific Gravity for Fresh (F-MSW, F-P25, and F-R25) and Low-Degraded, Medium-Degraded, and High-Degraded Decomposed Wastes Used in This Study

Material	F-MSW	F-P25	F-R25	Low degraded	Medium degraded	High degraded
Cellulose (%)	19.6	4.8	22.5	4.4	10.1	12.5
Hemicellulose (%)	5.4	1.5	5.4	1.6	4.0	4.3
Lignin (%)	28.8	6.6	28.6	43.5	30.6	33.1
(Cellulose + hemicellulose)/lignin	0.87	0.95	0.98	0.14	0.46	0.51
Volatile solids (%)	52.9	16.5	66.4	25.6	56.7	53.8
Biochemical methane potential (mL-CH_4/g-dry)	51.4	12.0	43.8	12.4	12.0	9.3
Biochemical methane potential/volatile solids (mL-CH_4/g-VS)	97.3	72.7	66.0	48.3	21.2	17.3
Reactor methane yield (L-CH_4/kg-dry)	NA	NA	NA	5.3	14.3	18.7
Specific gravity	1.34	NM	NM	1.65	1.80	1.90

Note: The cumulative methane yield from the laboratory anaerobic reactors is listed for decomposed wastes; NA = not applicable; NM = not measured.

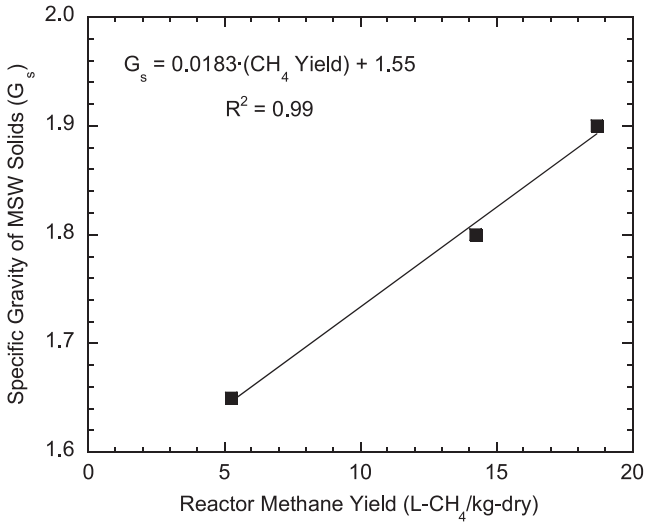

Fig. 2. Relationship between specific gravity (G_s) and reactor methane yield for decomposed wastes (LD, MD, and HD) prepared for this study

loads in the 64- and 100-mm cells. Dead weights were placed on the loading system manually. Displacement was recorded using LVDTs (30 ± 0.006 mm) from Omega Engineering, Inc. (Stamford, Connecticut, LD621-30) connected to a Campbell Scientific (CSI) CR23X Micrologger (Campbell Scientific, Inc., Logan, Utah).

Specimens

The initial γ_d and w_d of the compression specimens are presented in Table 3. All specimens were compacted via hand tamping in three layers of equal thickness to achieve uniform unit weights. The target γ_d and w_d for F-MSW were intended to corresponded to average initial conditions measured in the DTBE (γ_d = 6.3 kN/m^3 and w = 33%). However, a lower initial γ_d was obtained for F-MSW in the laboratory owing to difficulty in adequately densifying the reconstituted material. Hanson et al. (2010) also report lower waste unit weights achieved in laboratory experiments compared with unit weights in field-scale experiments compacted following typical operations of full-scale landfills.

The γ_d for F-P25 and F-R25 were selected to represent the relative γ_d of each waste fraction in the composite F-MSW. The dry unit weights for the F-P25 and F-R25 were computed assuming the volume of voids in F-MSW could be segregated into voids associated with the F-P25 and F-R25 fractions in proportion to the solid volume of each fraction (Bareither 2010).

The initial γ_d and w_d of the LD, MD, and HD specimens (Table 3) were the waste properties at the end of reactor operation after waste decomposition. Each reactor was operated under a 2-kPa vertical stress that simulated the interim cover soil of an operational bioreactor landfill. Thus, the γ_d and w_d of the decomposed waste were representative of superficial waste that was not densified by additional waste filling and subsequent stress increase.

The maximum particle size was 4.75 mm for the 64-mm cell, 9.5 mm for the 100-mm cell, and 25.4 mm for the 305-mm cell, corresponding to a cell diameter-to-maximum particle size ratio between 10 and 13. The F-MSW and F-R25 specimens in the 305-mm cells were reconstituted from material passed through a 25-mm screen. Fresh waste specimens in the 64- and 100-mm cells were reconstituted from sorted materials from the F-P25 analysis (Bareither et al. 2010b) as well as from shredded materials passed through 4.75- and 9.5-mm sieves. The specimens in all compression cells were prepared with a diameter-to-thickness ratio of approximately 2 to diminish the influence of sidewall friction. The waste composition (Table 1) and initial γ_d and w_d (Table 3) were similar for all three test scales.

A specimen of each fresh and decomposed waste used in the 305-mm compression cells was compacted with modified Proctor effort (ASTM 2009) to obtain a reference dry unit weight ($\gamma_{d\text{-MC}}$) and void ratio (e_{MC}). These specimens were compacted in a 152-mm-diameter compaction mold at water contents similar to those used for the compression specimens (Table 3). The following $\gamma_{d\text{-MC}}$ were obtained: 7.8 kN/m^3 for F-MSW; 5.7 kN/m^3 for F-R25; 13.3 kN/m^3 for F-P25; 8.5 kN/m^3 for LD; 8.7 kN/m^3 for MD; and 7.9 kN/m^3 for HD.

Procedures

The target temperature range for all compression tests was 45–48°C, which was the average temperature range in the DTBE prior to leachate dosing (Bareither et al. 2012). Flexible silicone rubber heaters (25 mm wide by 1.8 m long) were wrapped around the 305-mm cells for temperature control. Type-T thermocouples (Omega Engineering, Inc., Stamford, Connecticut) were used to monitor the waste temperatures. The temperatures were recorded and controlled with a CSI CR23X Micrologger connected with an AM25T thermocouple multiplexer.

Test cells containing the 64- and 100-mm waste specimens were placed inside an insulated box equipped with a 1-kW electric heater and a fan to promote air circulation. Type-T thermocouples (Omega Engineering, Inc., Stamford, Connecticut) were used to monitor the air temperatures inside the box and the waste temperatures within the test specimens. The temperature measurements were recorded with a CSI CR23X Micrologger connected with an AM25T thermocouple multiplexer.

Compression tests in the 305-mm cells were conducted within two stress ranges. The low-stress range (8–64 kPa) was similar to the stress range from the DTBE (20–67 kPa); the high-stress range (12–400 kPa) represents stresses anticipated in a 40-m-thick landfill. Compression tests in the 64- and 100-mm cells were only conducted in the low-stress range (9–68 kPa). In all compression tests, a seating load (i.e., ~4 kPa for low stress and ~6 kPa for high stress) was applied for the first 3 days to allow waste specimens to equilibrate. Incremental stresses were applied daily at a load increment ratio of 1. Additional effective stress owing to matric suction (Breitmeyer 2011) was negligible (~1 kPa) for all compression tests conducted in this study.

Determining End of Immediate Compression

Assessing immediate compression requires definition of the strain at which immediate compression ends and time-dependent compression begins; i.e., the end-of-immediate compression strain (ε_{EOI}). Methodologies used in soil mechanics for identifying transitions between primary and secondary consolidation (i.e., Casagrande's and Taylor's curve fitting techniques based on Terzaghi's one-dimensional theory of consolidation) are not applicable to MSW because the waste is unsaturated and excess pore pressure is not dissipating. An alternative method based on a first-order rate equation (FORE) procedure presented in Handy (2002) was adapted in this study to determine ε_{EOI} for MSW in a consistent manner.

The incremental loading relationships of strain versus time for F-MSW in 305-mm compression cells at both low-stress (8–64 kPa) and high-stress (12–400 kPa) ranges are shown in Fig. 4. A rapid accumulation of strain occurs immediately after each load application (immediate compression), which is followed by a diminishing

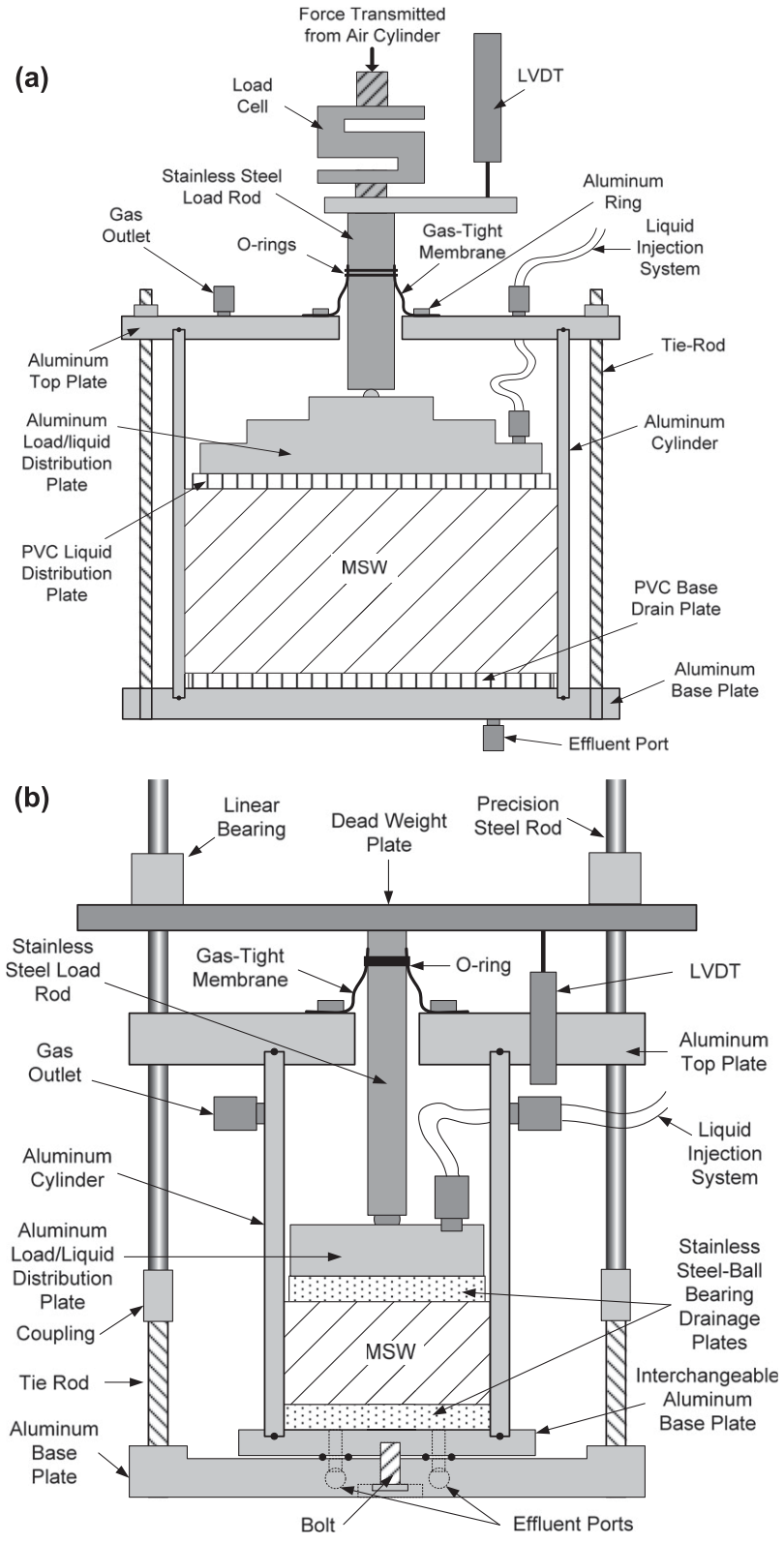

Fig. 3. Schematics of the (a) 305-mm-diameter compression cell and (b) 64- and 100-mm-diameter compression cells used in this study

rate of strain (mechanical creep). This behavior occurred in all tests conducted in this study and has been reported by others (Rao et al. 1977; Jessberger and Kockel 1995; Kavazanjian et al. 1999; Landva et al. 2000; Vilar and Carvalho 2004; Durmusoglu et al. 2006; Chen et al. 2010a).

An example of a strain versus time relationship from a single stress increment (0–24 h) for F-MSW is presented in Fig. 5. The FORE method was used following the recommendations given in Handy (2002) and coupled with a semilogarithmic equation to determine the transition between immediate compression and

Table 3. Laboratory Compression Test Summary

Waste	Cell diameter (mm)	Stress range (kPa)	Dry weight water content (%)	Dry unit weight (kN/m^3)	Test specific		Combined 305-mm data sets (25–100 kPa)	
					C_c'	R^2	C_c'	R^2
F-MSW	64	9–68	31.3	5.60	0.0911	0.959	—	—
	100	6–68		5.71	0.187	0.984	—	—
	305	8–64		5.61	0.162	0.986	0.224	0.995
		12–400		5.82	0.236	0.992		
	2,440[a]	20–67	33.0	6.30	0.229	0.995	—	—
F-P25	64	9–68	29.0	7.99	0.115	0.950	—	—
	100	10–68		8.12	0.188	0.987	—	—
	305	4–64	28.1	8.38	0.251	0.999	0.244	0.929
		6–400		8.53	0.234	0.997		
F-R25	64	9–68	28.7	4.37	0.0925	0.994	—	—
	100	10–68		4.26	0.215	0.980	—	—
	305	4–64		4.47	0.210	0.980	0.283	0.997
		6–400		4.30	0.280	0.994		
LD	305	8–64	46.4	6.62	0.183	0.988	0.231	0.998
		12–400		6.77	0.235	0.995		
MD	305	8–64	55.5	6.42	0.173	0.986	0.249	0.989
		12–400		6.63	0.257	0.994		
HD	305	8–64	62.9	6.52	0.193	0.986	0.229	0.982
		12–400		6.37	0.234	0.994		

Note: The water content and dry unit weight represent the specimen properties after 3 days of seating load application and temperature equilibration (DTBE included for comparison).
[a]DTBE.

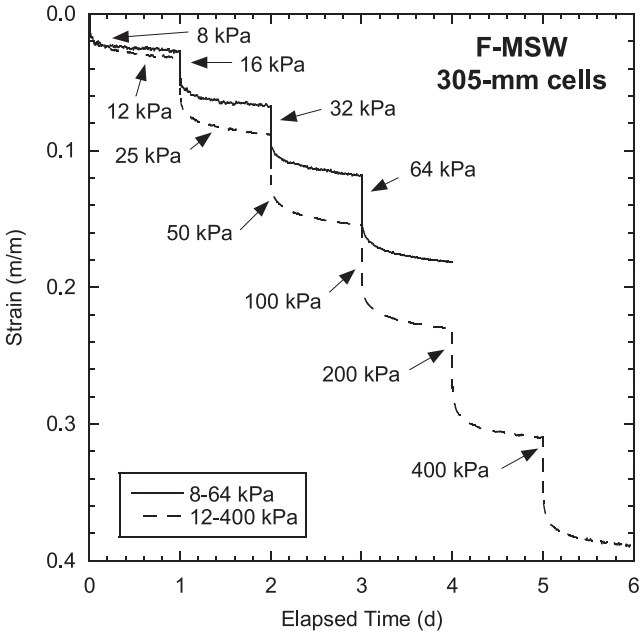

Fig. 4. Incremental loading relationships of compression strain versus time for F-MSW in 305-mm-diameter compression cells at low-stress (8–64 kPa) and high-stress (12–400 kPa) ranges

mechanical creep. The FORE and semilogarithmic equation are both applicable to representing physical compression processes (Handy 2002). The FORE simulates the physical process (i.e., mechanical creep) and the departure from that particular process, whereas the semilogarithmic equation simulates a continuous physical process with respect to the logarithm of time (i.e., constant mechanical creep ratio C_α'). Thus, the data overlapped by both the FORE and semilogarithmic equation in Fig. 5 are assumed to represent mechanical creep compression. Based on an assumption that mechanical creep can be represented by a single C_α' (e.g., El-Fadel and Khoury 2000; Gourc et al. 2010), the departure between the FORE and semilogarithmic predictions [Fig. 5(b)] coincides with the time at which compression behavior transitions from immediate compression to mechanical creep. Strain corresponding to this departure is taken as ε_{EOI}.

The FOREs were fit to experimental data sets encompassing the entire mechanical creep process (i.e., strain between 3 and 24 h) following the methodologies presented in Handy (2002). Semilogarithmic regressions were fit to the same data sets. Both relationships were fit by least-squares regression. After determining ε_{EOI} for each incremental load for a given experiment, C_c' was determined by linear least-squares regression of ε_{EOI} versus the logarithm of stress relationships.

The temporal relationships of compression strain during the first 60 days for the four settlement plates in the DTBE are shown in Fig. 6. The data from each settlement plate indicate that immediate compression occurred rapidly and transitioned to mechanical creep [Fig. 6(a)] in a manner similar to that observed in the laboratory (Figs. 4 and 5). The FORE and semilogarithmic relationships were fit to experimental data between 12 and 60 days. A larger data range was used for the DTBE analysis because immediate compression occurred slower in the DTBE than in the laboratory. The departure between the FORE and semilogarithmic relationship occurred between 12 and 16 days [Fig. 6(b)] for all four settlement plates. Bjarngard and Edgers (1990) reported initial settlements occurring within 2 days following load application for MSW field case histories. Although Bjarngard and Edgers (1990) did not determine a time for EOI compression, the rapid accumulation of settlement following load application is consistent with compression behavior in the DTBE (Fig. 6).

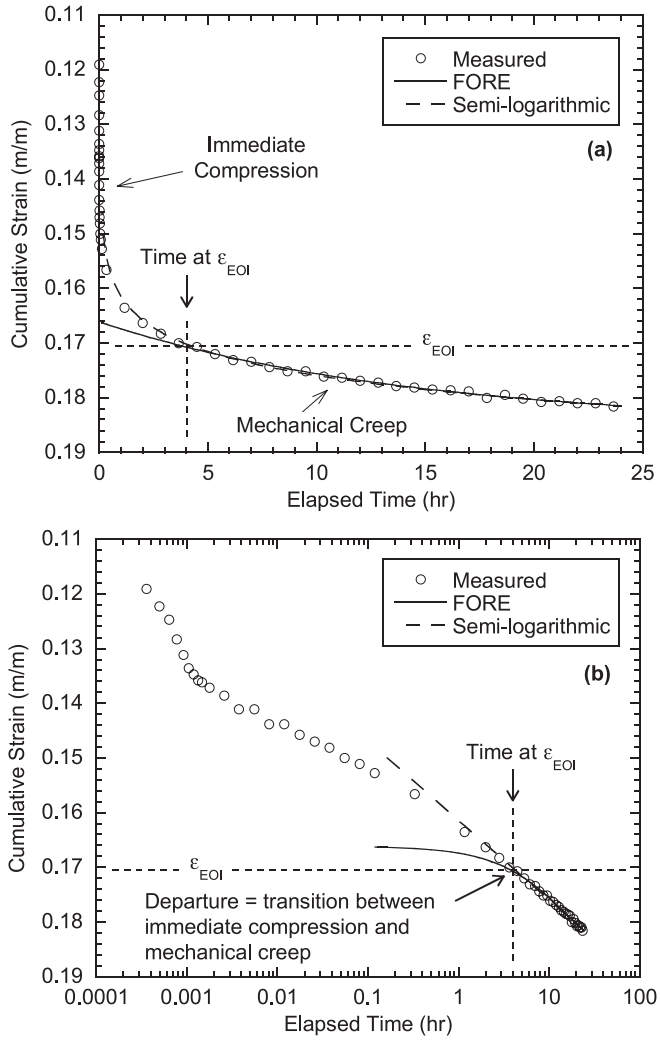

Fig. 5. Single incremental load relationship of strain versus time on (a) arithmetic and (b) logarithmic time scales for the 64-kPa stress on F-MSW; initial vertical stress for the data shown was 32 kPa; predicted strains by the FORE and semilogarithmic regression

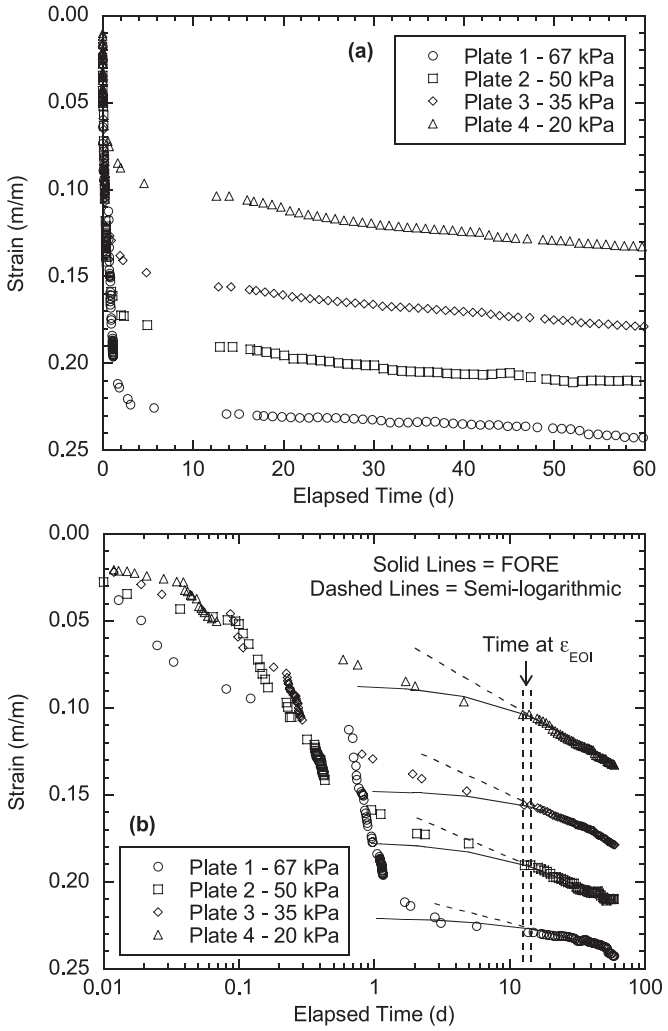

Fig. 6. Temporal relationships of compression strain on (a) arithmetic and (b) logarithmic time scales for the four settlement plates in the DTBE and predicted mechanical creep between 12 and 60 days based on FORE analysis and semilogarithmic regression

Immediate Compression Behavior

Effect of Scale

Strain versus time and ε_{EOI} versus stress relationships are shown in Fig. 7 for experiments conducted in 64-, 100-, and 305-mm cells on fresh waste (F-MSW, F-R25, and F-P25). A summary of the C_c' and corresponding coefficient of determination (R^2) for each compression test is given in Table 3. The ε_{EOI} versus stress relationship for the DTBE is also included in Fig. 7. Immediate compression occurred rapidly upon loading and then exhibited a transition to mechanical creep in each of the three fresh wastes [Figs. 7(a, c, and e)] in all three scales of laboratory compression cells. The least compression and smallest C_c' were obtained from the 64-mm cells. Comparable strains accumulated in the 100- and 305-mm cells for F-MSW and F-R25.

The accumulated strain and C_c' for F-R25 in the 100- and 305-mm cells [0.21 and 0.22, Fig. 7(d)] are more comparable to C_c' for the DTBE relative to F-MSW and F-P25. The lower C_c' for F-MSW in the 100- and 305-mm cells compared with the DTBE [Fig. 7(b)] is attributed to curvature of the strain versus log-stress relationship (i.e., C_c' increasing with stress). These lower C_c' at low stress appear to be a result of the higher precompression stress present in the waste fabric induced during compaction (discussed subsequently).

Lower immediate compression strains in all 64-mm cells are attributed to changes in water content that occurred during testing. No drainage from the specimens occurred prior to or during loading. However, examination of the test specimens indicated they dried (e.g., final $w_d < 1\%$ for F-P25), possibly owing to the heat applied to maintain waste temperatures. Stoltz et al. (2010) conducted compression tests in 270-mm-diameter cells on waste at varying water contents and report their smallest C_c' for waste with the lowest water content.

Effects of Stress

The relationships between C_c' and stress for the three fresh wastes and the three decomposed wastes from the tests in 305-mm compression cells are shown in Fig. 8. In Fig. 8, C_c' are computed incrementally with respect to the accumulated strain for each additional stress increment ($\Delta\varepsilon/\Delta\log\sigma$) and are graphed with respect to the larger stress. The dashed lines in Fig. 8 capture the general behavior of C_c' versus stress. F-MSW and F-R25 specimens in Fig. 8(a) and the three decomposed wastes (LD, MD, and HD) in Fig. 8(b)

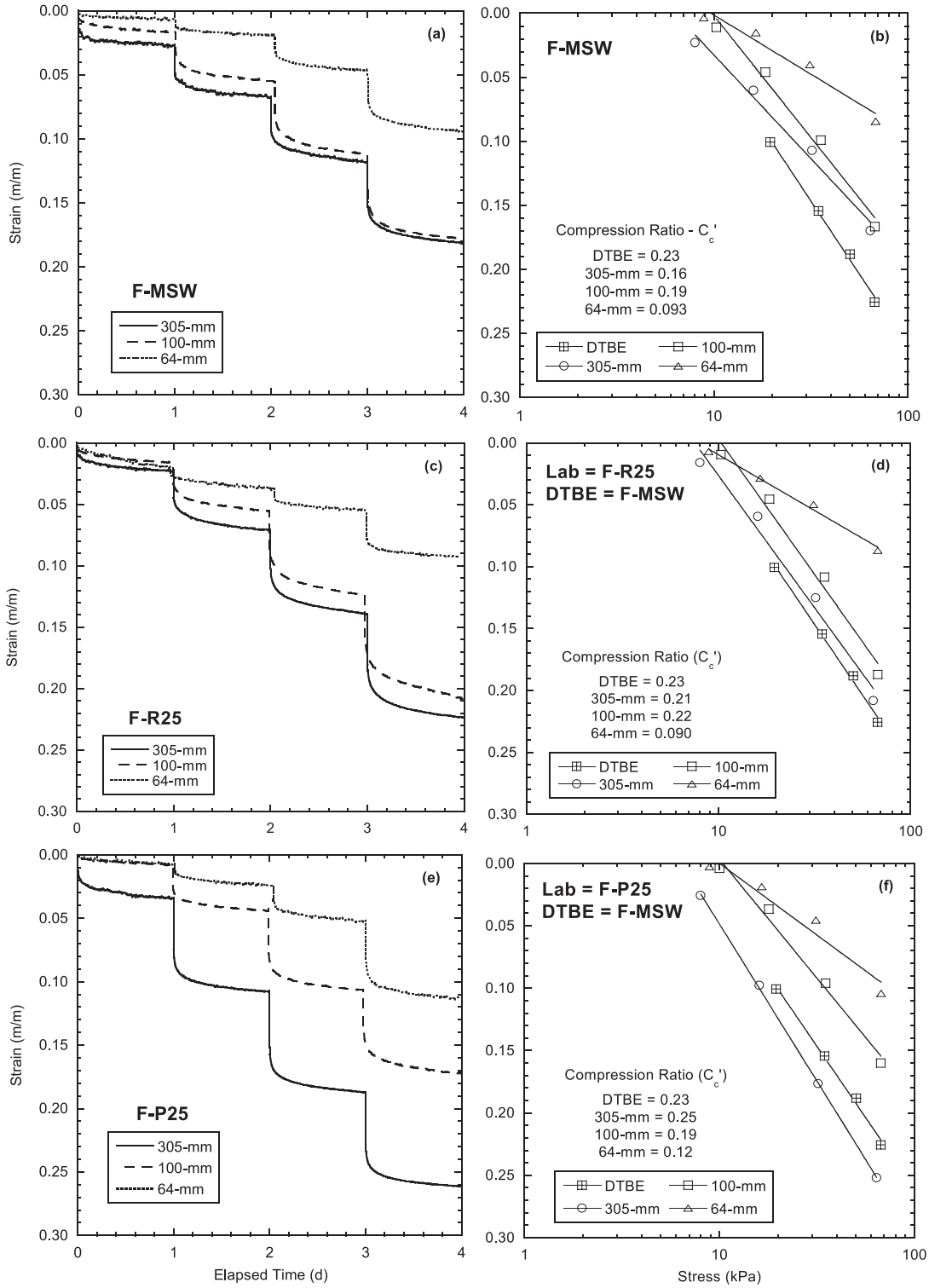

Fig. 7. (a) Incremental loading relationships of strain versus time for F-MSW; (b) end of immediate compression strain versus stress for F-MSW; (c) incremental loading relationships of strain versus time for F-R25; (d) end of immediate compression strain versus stress for F-R25; (e) incremental loading relationships of strain versus time for F-P25; and (f) end of immediate compression strain versus stress for F-P25 (in 64-, 100-, and 305-mm-diameter compression cells)

depict similar trends, with C_c' increasing with stress and then leveling off at approximately 100 kPa. The data from the DTBE also fall in these same bands [Figs. 8(a and b)]. In contrast, C_c' for F-P25 [Fig. 8(a)] is approximately constant between 16 and 100 kPa, ranging from 0.24 to 0.26, and then decreases with increasing stress.

The similarities in the C_c' versus stress relationships between the DTBE and F-MSW and F-R25 as well as the three decomposed wastes, suggest that bulky waste constituents (e.g., paper, plastic, wood, etc.) must be included when evaluating the immediate compression behavior of MSW. These bulky waste constituents

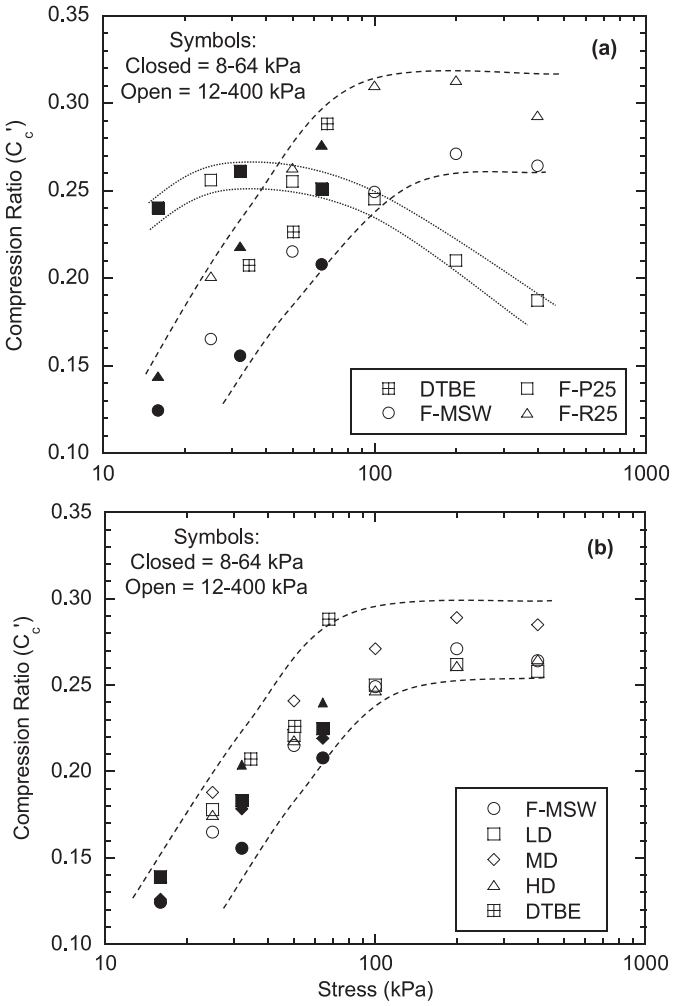

Fig. 8. Relationships of compression ratio versus stress for (a) fresh wastes (F-MSW, F-P25, and F-R25) and (b) decomposed wastes (LD, MD, and HD) at low- and high-stress ranges in 305-mm-diameter compression cells (DTBE data included for comparison)

create a waste with higher compressibility compared with the soil-like F-P25, which contained > 85% soil, gravel, and inert material (Table 1). The C_c' versus stress relationship for F-P25 [Fig. 8(b)] suggests the waste matrix is stiffening with increased stress, which is not representative of the DTBE or the other wastes containing bulky constituents.

The different C_c' versus stress relationship for F-P25 (Fig. 8) is attributed to waste segregation and a lower compaction effort required to obtain the initial specimen γ_d (Table 3). As mentioned previously, the target γ_d for F-MSW was the average γ_d for the DTBE, and γ_d for F-R25 and F-P25 were selected to represent the approximate γ_d of each fraction in the composite F-MSW. The F-P25 specimen required less compaction effort to attain the target γ_d (~8.45 kN/m^3), resulting in a lower initial γ_d relative to that obtained by modified Proctor compaction ($\gamma_{d\text{-MC}}$ = 13.3 kN/m^3). This compaction effort produced a more compressible waste at low stress (i.e., larger C_c'), followed by a decreasing C_c' trend with stress increase due to waste segregation that removed bulky waste constituents [Fig. 8(a)]. A similar effect of decreasing C_c' with increasing stress was reported by Chen et al. (2010a) and attributed to the low compaction energies used to achieve their target γ_d.

Higher compaction efforts were required to achieve the target γ_d in the F-MSW, F-R25, LD, MD, and HD 305-mm compression specimens. This compaction effort resulted in a higher precompression stress in the initial waste fabric and essentially produced overconsolidated waste specimens. An increase in C_c' with stress has also been reported by Stoltz et al. (2010) for laboratory-prepared MSW specimens. Thus, C_c' should be evaluated in either (1) a broad stress range that encompasses expected field stresses or (2) a stress range where C_c' is approximately constant.

Relationships of ε_{EOI} versus stress for fresh and decomposed wastes in 305-mm compression cells at both low-stress (8–64 kPa) and high-stress (12–400 kPa) ranges are shown in Fig. 9. Data sets from the low- and high-stress ranges for a given waste overlap [e.g., F-MSW in Fig. 9(a)] indicate that the compression behavior for low- and high-stress range specimens is consistent. Thus, the data sets were combined and a single C_c' was obtained by nonlinear regression for each combined data set (F-MSW, F-P25, F-R25, LD, MD, and HD) in the stress range of 25–100 kPa (Fig. 9 and Table 3), which is comparable to the range in the DTBE (20–67 kPa).

The C_c' for F-MSW determined from the combined 305-mm data sets was 0.22 (Table 3). The compression curve for the DTBE was essentially parallel to this combined laboratory data set [Fig. 9(a)], with a C_c' = 0.23. This suggests that immediate compression of MSW at field scale can be assessed via laboratory compression experiments in 305-mm-diameter cells following the procedures described herein. The C_c' determined for F-R25 (0.28) and F-P25 (0.24) are slightly larger compared with F-MSW in the DTBE (Table 3). The larger C_c' for F-R25 is attributed to a larger fraction of bulky, organic waste (OW) (Table 1), whereas the larger C_c' for F-P25 is likely a result of the lower compaction effort used to achieve the target γ_d.

Nearly identical ε_{EOI} versus stress relationships were determined for the four wastes at various states of decomposition [Fig. 9(b)]. The average C_c' for stresses between 25 and 100 kPa fall within a narrow range (0.22–0.25), and are also similar to C_c' for the DTBE (0.23). This similarity in C_c' suggests that waste decomposition has a negligible effect on the immediate compression behavior. This finding is relevant to decomposed waste specimens reconstituted in laboratory compression cells.

Sustained Loading and Waste Decomposition

To assess the impact of sustained loading and waste decomposition on immediate compression behavior, F-MSW was subjected to leachate recirculation in a 305-mm cell under 64-kPa creep stress for 365 days. Waste decomposition during this constant stress phase generated 7.6 L-CH_4/kg-dry, which is between the reactor methane yields for LD and MD (Table 2). Following 365 days of compression, the 64-kPa stress was removed from the specimen, reapplied incrementally from 8 to 64 kPa, and then increased to 100, 200, and 400 kPa.

The relationships of ε_{EOI} versus stress for this F-MSW specimen are shown in Fig. 10(a) along with data from the F-MSW specimen tested in the higher stress range (12–400 kPa). The roman numerals included in Fig. 10 document the experimental progression for the F-MSW specimen subjected to sustained loading as follows: (I) incremental loading from 8 to 64 kPa; (II) sustained loading for 365 days under 64 kPa; (III) unloading followed by reloading from 8 to 64 kPa; and (IV) incremental loading to 100, 200, and 400 kPa. Mechanical creep and biocompression contributed an additional 20% strain in the F-MSW specimen under a constant 64 kPa stress for 365 days [Fig. 10(a)], and γ_d increased from 6.7 to 8.3 kN/m^3 (accounting for solid loss due to decomposition). The initial C_c' for F-MSW between 8 and 64 kPa was 0.16. The recompression ratio (C_r') following 365 days of sustained loading was 0.015 (Fig. 10), or 10.7 times lower than C_c'. The C_c'/C_r' ratios for fine-grained soils are of

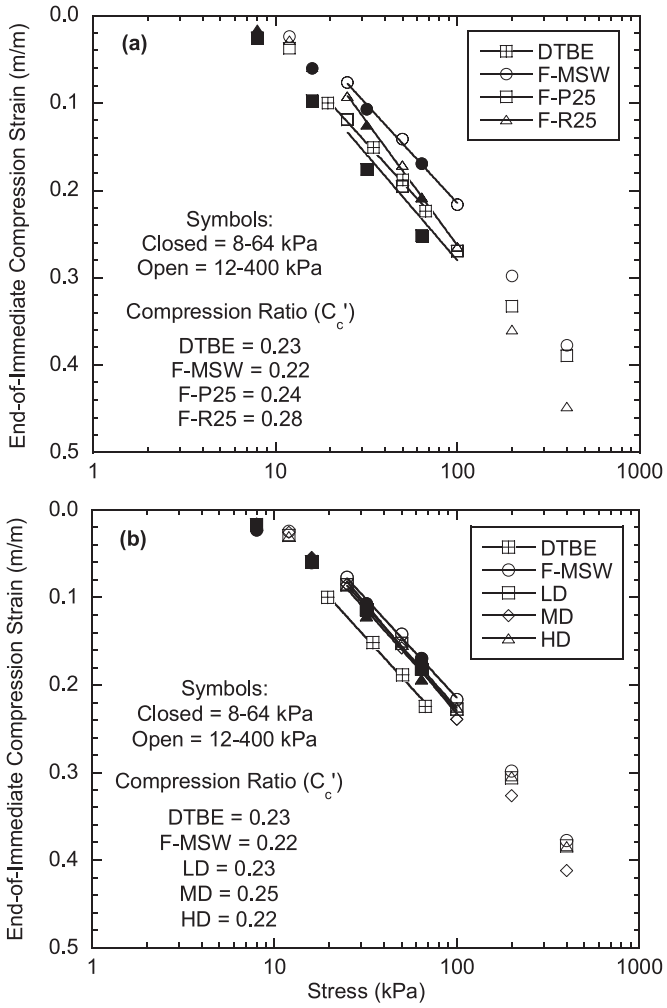

Fig. 9. Relationships of end-of-immediate compression strain versus stress for (a) fresh wastes (F-MSW, F-P25, and F-R25) and (b) decomposed wastes (LD, MD, and HD) at low- and high-stress ranges in 305-mm-diameter compression cells; immediate compression ratio (C_c') computed in the stress range of 25–100 kPa for laboratory experiments (DTBE data included for comparison)

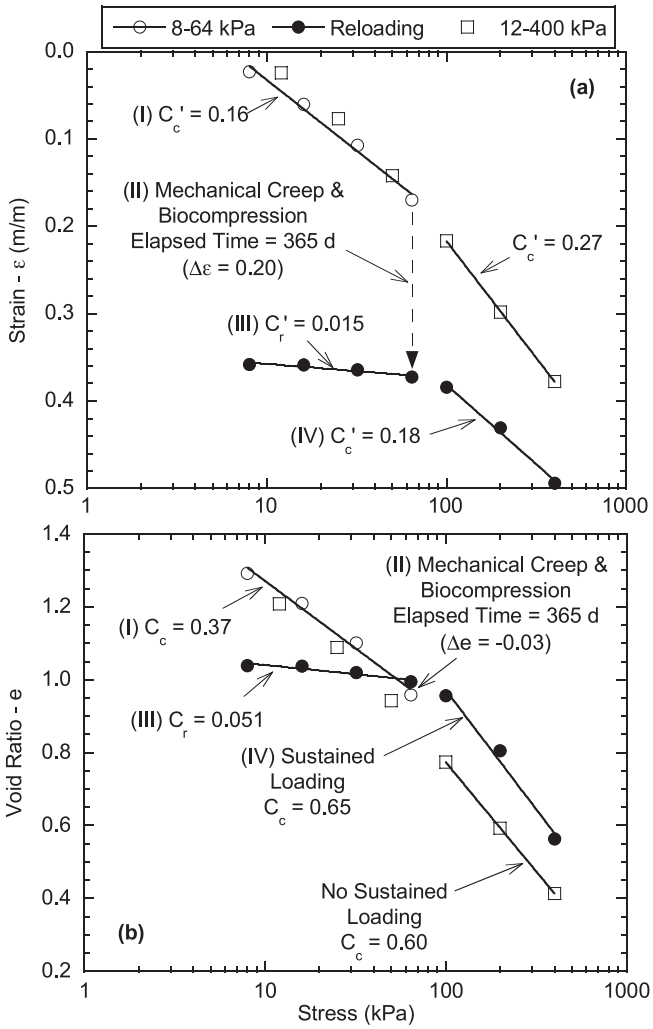

Fig. 10. (a) Strain versus stress relationship and (b) void ratio versus stress relationship for F-MSW in 305-mm compression cells for low-stress (8–64 kPa) and high-stress (12–400 kPa) ranges; roman numerals identify experimental progression of the sustained loading experiment: (I) incremental loading from 8 to 64 kPa; (II) mechanical creep and biocompression (i.e., sustained loading) for 365 days at 64 kPa; (III) unloading followed by reloading from 8 to 64 kPa; and (IV) incremental loading to 100, 200, and 400 kPa

similar magnitude (Holtz and Kovacs 1981). The C_c' in the stress range of 100–400 kPa for F-MSW without sustained loading was 0.27; however, C_c' decreased to 0.18 following 365 days of sustained loading [Fig. 10(a)]. A similar reduction in C_c' following sustained loading and waste decomposition under 150 kPa, relative to fresh waste, was reported by Chen et al. (2010b).

The relationships of ε_{EOI} versus stress presented in Fig. 10(a) are reproduced in Fig. 10(b) in terms of the void ratio (e) versus stress. The compression indices C_c and C_r were obtained by regression of e on the logarithm of stress. Void ratios for F-MSW subjected to sustained loading were computed by estimating G_s from methane yield using the relationship in Fig. 2. The strain accumulated due to mechanical creep and biocompression during sustained loading ($\Delta\varepsilon = 0.20$) corresponds to an increase in void ratio from 0.96 to 0.99 ($\Delta e = -0.03$). This change in void ratio is a result of waste decomposition, which decreases the solid volume, increases the void volume, and results in higher void ratios for comparable waste volumes (McDougall et al. 2004).

Waste decomposition in the F-MSW specimen subjected to sustained loading resulted in higher void ratios compared with the F-MSW specimen without sustained loading for stress >50 kPa [Fig. 10(b)]. At stresses of 100 kPa and higher, C_c for F-MSW with sustained loading (0.65) was greater than C_c for F-MSW without sustained loading (0.60). This disparity between C_c [Fig. 10(b)] and C_c' [Fig. 10(a)] for F-MSW with and without sustained loading is a result of waste decomposition and removal of compressible organic solids from the F-MSW specimen subjected to sustained loading.

The solid volume is compressible in MSW but becomes less compressible as decomposition progresses. For MSW decomposed under a sustained load, removal of organic solids simultaneously creates a higher void ratio and stiffer solid matrix (Fig. 10). This phenomenon is caused by the less compressible and less biodegradable waste matrix remaining intact while decomposition progresses. In contrast, reconstituting decomposed MSW (e.g., LD, MD, and HD compression tests) redistributes the remaining bulky waste constituents and organic solids to create a waste matrix with higher compressibility potential, similar to fresh MSW [Fig. 9(b)].

Although immediate compression of decomposed MSW differs for sustained loading and reconstituted specimens, the compression

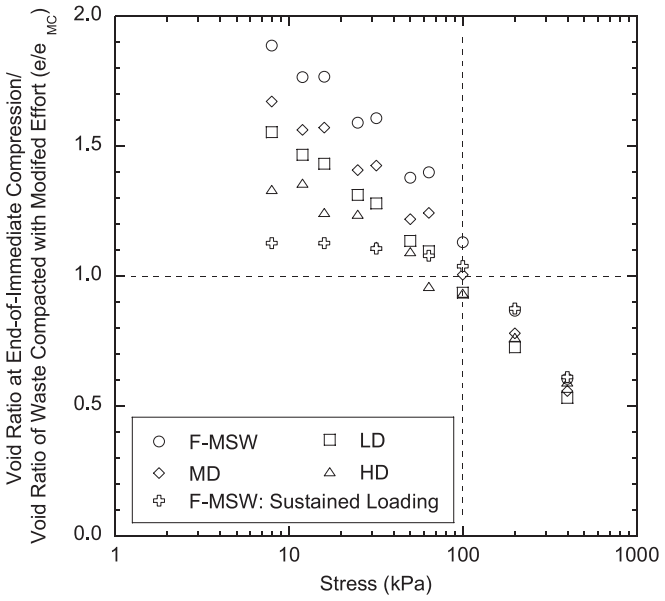

Fig. 11. Ratio of the void ratio during compression (e) to the void ratio of waste compacted with modified compaction effort (e_{MC}) versus applied vertical stress for F-MSW, LD, MD, HD, and F-MSW subjected to sustained loading in 305-mm-diameter compression cells

mechanisms are similar. The relationships between void ratio at EOI compression normalized to void ratio of waste compacted with modified effort (e_{MC}) for F-MSW, LD, MD, and HD are shown in Fig. 11. Data are also shown for F-MSW subjected to sustained loading. The e_{MC} for F-MSW under sustained loading was computed from G_s determined from Fig. 2 and $\gamma_{d\text{-MC}}$ averaged from LD and MD because comparable decomposition occurred. Data in Fig. 11 indicate that regardless of the initial specimen compaction, waste decomposition, or sustained loading, immediate compression behavior becomes similar as stress increases. This suggests that the differences in the waste matrix induced by decomposition and/or sustained loading are ameliorated as the stress increases.

The trends in Fig. 11 also suggest that the modified compaction effort is representative of waste void ratios (unit weights) at approximately 100-kPa vertical stress. The modified compaction effort may be applicable for preliminary estimates of waste unit weight and void ratio that can be linked to unit weight profiles (e.g., Zekkos et al. 2006) and waste behavior (e.g., hydraulic conductivity in Breitmeyer 2011). These relationships can provide a means of parameterizing bioreactor performance models (e.g., McDougall 2007). Additionally, geotechnical characteristics (e.g., compression, hydraulic conductivity, shear strength) assessed on waste compacted with modified effort can be linked to a reference depth within a landfill.

Estimating C_c' from Waste Properties

Data from the laboratory compression experiments on MSW in this study and the literature were compiled to develop a method to estimate C_c' that accounts for waste properties. Summary of the data are given in Tables 4–6. The small-scale data are from compression cells with a diameter (d) between 63 and 95 mm (Table 4), mesoscale data are for d between 190 and 365 mm (Table 5), and large-scale data are for d between 600 and 2,000 mm (Table 6).

The analysis was limited to studies that presented ε_{EOI} versus stress relationships for individual experiments. Analyses were not conducted to determine ε_{EOI}, except in one case. In Chen and Lee (1995), ε_{EOI} was assumed to correspond to strain at the end of daily incremental stress applications because ε_{EOI} was not reported and the ε_{EOI} method used in the current study was not applicable to the data. The ε_{EOI} versus stress data from each study were analyzed independently by the writers using least-squares linear regression to provide consistency in determining C_c'. Thus, minor differences exist between C_c' reported in the references and those summarized in Table 4–6.

No single waste characteristic was found to consistently influence C_c'. However, C_c' is sensitive to w_d, γ_d, and the percent of biodegradable OW. These variables were combined into the dimensionless waste compressibility index (WCI), which is defined as

$$\text{WCI} = w_d \cdot \left(\frac{\gamma_w}{\gamma_d}\right) \cdot \left(\frac{\text{OW}}{100 - \text{OW}}\right) \tag{2}$$

where γ_w = unit weight of water, which is used to nondimensionalize γ_d. The percent of biodegradable OW is the sum of the percent of paper, cardboard, food waste, and yard waste on a dry mass basis.

The relationship between C_c' and WCI is presented in Fig. 12. Data from the current study are designated as 100 and 305 mm corresponding to the diameter of the compression tests. The regression of C_c' on WCI included all data except the two outliers identified in Fig. 12 (68 individual points), and resulted in $R^2 = 0.45$. Both regression coefficients were significant at a 5% significance level (i.e., p statistics $\ll 0.05$). The regression indicates that larger C_c' are associated with larger WCIs, which corresponds to waste with higher w_d, lower γ_d, and/or higher OW. Sowers (1973) identified larger compression indices for materials with higher organic contents, Landva et al. (2000) and Chen et al. (2009) indicated that C_c' decreases with increasing waste density, and Dixon et al. (2008) indicated that C_c' decreases with an increase in the percent of incompressible materials (e.g., nonorganic materials). Thus, the material parameters used in the WCI and the influence of these parameters on C_c' shown in Fig. 12 are consistent with the literature.

The dashed lines in Fig. 12 correspond to ± 2 SD (σ) from the regression line. Here, C_c' can be predicted to be ± 0.087 for a given WCI. The C_c' obtained for a given WCI, combined with the upper and lower bounds corresponding to $\pm 2\sigma$, can be used to define a range of expected immediate compression for MSW.

The data in Fig. 12 also suggest that the test scale is not a significant factor influencing immediate compression behavior. Each experimental scale identified in Fig. 12 (i.e., small, meso, and large) encompasses nearly the entire range of the WCI and exhibits a similar trend of increasing C_c' with increasing WCI. Future research focusing on variations in the material properties included in the WCI and assessing the corresponding impact on C_c' will help strengthen this relationship and improve predictive capabilities.

Summary and Conclusions

This paper presents the findings from a study conducted to evaluate scale effects, stress, waste segregation, and waste decomposition on the immediate compression behavior of MSW. Scale effects were investigated in compression cells with diameters of 64, 100, and 305 mm. Effects of waste segregation were evaluated by using three size-differentiated fractions of fresh waste (F-MSW, F-P25, and F-R25). Decomposition effects were evaluated by decomposing fresh waste (F-MSW) in laboratory anaerobic reactors to three different states of decomposition (LD, MD, and HD) and subsequently testing the decomposed wastes in 305-mm compression cells.

Table 4. Summary of Small-Scale (63 mm < Cell Diameter < 95 mm) Compression Tests Used for Predicting the Compression Ratio

Reference	Waste description	Diameter (mm)	Dry weight water content (%)	Dry unit weight (kN/m^3)	Degradable organics (%)	Other waste (%)	Waste compressibility index	C_c'	R^2
Gabr and Valero (1995)	15–30-year-old waste borehole samples (United States)	64	108.0	5.61	2	98	0.039	0.200	0.998
		64	100.0	9.81	2	98	0.020	0.173	0.996
		64	135.0	8.18	2	98	0.033	0.156	0.975
		64	114.3	6.33	2	98	0.036	0.166	0.995
		64	114.3	7.85	2	98	0.029	0.174	0.999
		64	114.3	7.01	2	98	0.033	0.166	0.996
Chen et al. (2009)	Waste recovered from various depths in boreholes (China)	95	107.1	4.57	43	57	1.734	0.307	0.996
		94	51.8	7.15	29	71	0.290	0.202	0.995
		94	50.0	5.93	28	72	0.322	0.234	0.962
		82	49.1	9.14	26	74	0.185	0.143	0.979
		82	50.0	8.05	22	78	0.172	0.151	0.980
		82	98.2	9.35	23	77	0.308	0.072	0.969
Reddy et al. (2009c)	Waste obtained from working phase (United States)	63	44.0	2.89	28	72	0.592	0.274	0.994
		63	60.0	3.97	28	72	0.588	0.246	0.986
		63	80.0	4.04	28	72	0.770	0.325	0.989
		63	100.0	3.78	28	72	1.030	0.235	0.984
Reddy et al. (2009a)	1.5-year-old waste with leachate recirculation (United States)	63	44.0	5.20	23	77	0.251	0.190	0.976
		63	60.0	5.20	23	77	0.342	0.194	0.995
		63	80.0	5.20	23	77	0.456	0.199	1.000
		63	100.0	5.20	23	77	0.570	0.241	0.997
Reddy et al. (2009b)	Prepared waste to simulate typical U.S. composition	63	116.0	5.22	60	40	3.269	0.331	0.996
		63	116.0	4.90	60	40	3.485	0.240	0.985
		63	116.0	5.44	60	40	3.138	0.210	0.987
		63	116.0	4.62	60	40	3.694	0.319	0.993
		63	116.0	4.12	60	40	4.143	0.117	0.987

Table 5. Summary of Mesoscale (190 mm < Cell Diameter < 365 mm) Compression Tests Used for Predicting the Compression Ratio

Reference	Waste description	Diameter (mm)	Dry weight water content (%)	Dry unit weight (kN/m^3)	Degradable organics (%)	Other waste (%)	Waste compressibility index	C_c'	R^2
Chen and Lee (1995)	5- to 15-year-old refuse (Taiwan)	305	56.3	4.39	50	50	1.267	0.253	0.994
Vilar and Carvalho (2004)	15-year-old waste from boring (Brazil)	365	63.1	4.89	14	86	0.206	0.236	0.997
		365	95.4	5.36	14	86	0.284	0.222	0.994
		365	132.9	5.63	14	86	0.377	0.325	0.988
Stoltz and Gourc (2007)	1-year-old waste (France)	270	56.0	4.71	20	80	0.291	0.260	0.997
Chen et al. (2010b)	Prepared waste to typical composition in China	190	44.4	5.47	56	44	1.026	0.204	0.994
		190	49.8	4.34	56	44	1.451	0.315	0.998
Stoltz et al. (2010)	Waste recovered from landfill (France)	270	22.6	4.02	54	46	0.647	0.269	1.000
		270	46.0	4.03	54	46	1.314	0.288	0.997
		270	60.7	4.07	54	46	1.717	0.280	0.998
		270	72.3	4.31	54	46	1.933	0.270	0.992
		270	75.2	3.99	54	46	2.169	0.333	0.998
		270	81.2	3.99	54	46	2.342	0.322	0.998
		270	90.7	3.87	54	46	2.702	0.373	1.000
		270	101.8	4.08	54	46	2.873	0.322	0.997
		270	118.0	3.94	54	46	3.446	0.296	0.999
		270	116.5	4.21	54	46	3.188	0.288	0.997

The compression behavior observed in laboratory experiments was compared with data from a field-scale experiment (DTBE) to assess the efficacy of reproducing field-scale compression behavior in the laboratory. Additionally, laboratory data from the literature were compiled to substantiate the results from this study and aid in creating a predictive tool for estimating the compression ratio (C_c') from waste composition and material properties.

Table 6. Summary of Large-Scale (600 mm < Cell Diameter < 2000 mm) Compression Tests Used for Predicting the Compression Ratio

Reference	Waste description	Diameter (mm)	Dry weight water content (%)	Dry unit weight (kN/m^3)	Degradable organics (%)	Other waste (%)	Waste compressibility index	C_c'	R^2
Rao et al. (1977)	Prepared waste to	610	30.0	1.79	70	30	3.827	0.208	0.966
	simulate typical U.S.	610	30.0	2.24	70	30	3.061	0.189	0.992
	composition	610	30.0	2.69	70	30	2.551	0.236	0.991
		610	30.0	3.14	70	30	2.187	0.227	0.992
Beaven and	Waste obtained from	2,000	51.0	4.32	57	43	1.543	0.184	0.996
Powrie (1995)	tipping face	2,000	112.0	3.53	57	43	4.141	0.289	0.990
	(England)	2,000	102.0	3.24	53	47	3.485	0.341	0.985
		2,000	151.0	2.45	56	45	7.533	0.389	0.984
		2,000	40.0	1.86	56	45	2.626	0.344	0.974
		2,000	71.2	5.30	37	63	0.774	0.263	0.996
Landva et al. (2000)	5-year-old waste (Canada)	600	15.6	9.00	47	53	0.148	0.157	0.993
	2-year-old waste (Canada)	600	18.8	7.49	29	71	0.099	0.209	0.996
	Prepared waste	600	53.1	5.16	8	92	0.088	0.205	0.994
	Prepared waste	600	51.3	5.02	13	88	0.143	0.184	0.982
	mixtures of 2- and 5-year-old waste (Canada)	600	51.3	5.02	13	88	0.143	0.172	0.962
Olivier et al. (2003)	Prepared waste	1,000	35.4	7.20	55	45	0.589	0.236	0.989
Olivier and Gourc (2007)	Prepared waste	1,000	43.4	4.17	55	45	1.248	0.271	0.945
		1,000	51.2	4.41	55	45	1.393	0.220	0.977

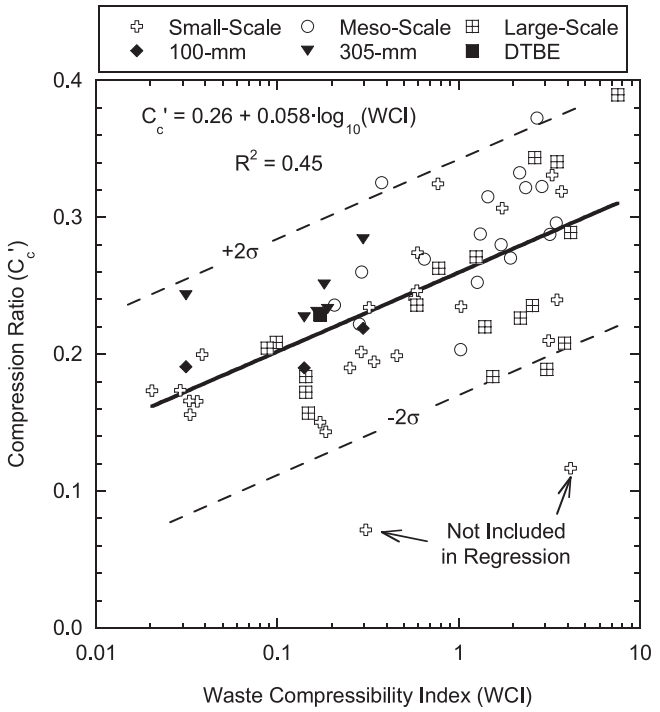

Fig. 12. Relationship between the C_c' and WCI; data from the literature segregated by diameter d of the compression cell: small-scale = 63 mm $< d <$ 95 mm, meso-scale = 190 $< d <$ 365 mm, and large-scale = 600 $< d <$ 2000 mm; tests conducted in this study included 100- and 305-mm-diameter compression cells.

The following conclusions are based on the study:

- The EOI compression strain (ε_{EOI}) was identified at shorter elapsed times in the laboratory compression tests (3–4 h) compared with the DTBE (12–16 days).
- The immediate compression ratio (C_c') was not constant with stress. Thus, C_c' should be evaluated in either (1) a broad stress range that encompasses field stress or (2) a stress range where C_c' is approximately constant.
- Segregating fresh waste and evaluating compression behavior on the fraction passing a 25-mm screen (P25) is not representative of field-scale behavior. Laboratory experiments that are applicable to field-scale compression behavior must include bulky waste constituents (material retained on a 25-mm screen in this study).
- The C_c' for F-MSW in a 305-mm cell was nearly the same as the C_c' in the DTBE (0.22 versus 0.23), within a comparable stress range. An appropriate field-scale C_c' can be determined in 305-mm compression cells following the procedures described in this study.
- A negligible effect of waste decomposition on C_c' was found when decomposed waste was reconstituted in laboratory compression cells. However, sustained loading coupled with waste decomposition decreased C_c' owing to removal of compressible organic solids and stiffening of the waste matrix.
- A logarithmic relationship between C_c' and WCI can be used to predict $C_c' \pm 0.087$ for a given WCI. The WCI is a function of dry weight water content, dry unit weight, and percent of biodegradable OW.

Acknowledgments

Financial support for this study was provided by the University of Wisconsin–North Carolina State University bioreactor partnership (www.bioreactorpartnership.org), which was sponsored by the U.S. National Science Foundation (Grant No. EEC-0538500) and a consortium of industry partners (CH2MHill; Geosyntec Consultants; Republic Services; Veolia Environmental Services; Waste Connections, Inc.; and Waste Management) through the National Science Foundation's Partnerships for Innovation Program. Additional thanks are extended to Professor Morton Barlaz (North Carolina State

University) for his prominent role in the overall project and Ronald Breitmeyer (Exponent, Inc.) for assistance with the laboratory testing.

References

ASTM. (2009). "Standard test methods for laboratory compaction characteristics of soil using modified effort." *D1557*, West Conshohocken, PA.

Bareither, C. A. (2010). "Compression behavior of solid waste." Ph.D. dissertation, Univ. of Wisconsin–Madison, Madison, WI.

Bareither, C. A., Benson, C. H., Barlaz, M. A., Edil, T. B., and Tolaymat, T. M. (2010a). "Performance of North American bioreactor landfills: I. Leachate hydrology and waste settlement." *J. Environ. Eng.*, 136(8), 824–838.

Bareither, C. A., Breitmeyer, R. J., Benson, C. H., Barlaz, M. A., and Edil, T. B. (2012). "Deer Track Bioreactor Experiment: A field-scale evaluation of municipal solid waste bioreactor performance." *J. Geotech. Geoenviron. Eng.*, 138(6), 658–670.

Bareither, C. A., Breitmeyer, R. J., Meyer, L. L., Benson, C. H., Edil, T. B., and Barlaz, M. A. (2010b). "Physical, chemical, and biological characterization of solid waste samples." *Proc., Global Waste Management Symp.*, Penton Media, New York, 1–9.

Beaven, R. P., and Powrie, W. (1995). "Determination of the hydrogeological and geotechnical properties of refuse using a large scale compression cell." *Proc., 5th Int. Sardinia Landfill Conf.*, CISA, Environmental Sanitary Engineering Centre, Cagliari, Italy, Vol. 2, 745–760.

Benson, C. H., Barlaz, M. A., Lane, D. T., and Rawe, J. M. (2007). "Bioreactor landfills in North America: Review of the state-of-the-practice." *Waste Manage.*, 27(1), 13–29.

Bjarngard, A., and Edgers, L. (1990). "Settlement of municipal solid waste landfills." *Proc., 13th Annual Madison Waste Conf.*, Univ. of Wisconsin–Madison, Madison, WI, 192–205.

Breitmeyer, R. J. (2011). "Hydraulic characterization of municipal solid waste." Ph.D. dissertation, Univ. of Wisconsin–Madison, Madison, WI.

Chen, R. H., Chen, K. S., and Liu, C. N. (2010a). "Study of the mechanical compression behavior of municipal solid waste by temperature-controlled compression tests." *Environ. Earth Sci.*, 61 (8), 1677–1690.

Chen, R. H., and Lee, Y. S. (1995). "Settlement analysis of a waste landfill." *Proc., 3rd Int. Symp. on Environmental Geotechnology*, CRC Press, Boca Raton, FL, 539–553.

Chen, Y., Ke, H., Fredlund, D. G., Zhan, L., and Xie, Y. (2010b). "Secondary compression of municipal solid wastes and a compression model for predicting settlement of municipal solid waste landfills." *J. Geotech. Geoenviron. Eng.*, 136(5), 706–717.

Chen, Y. M., Zhan, L. T., Wei, H. Y., and Ke, H. (2009). "Aging and compressibility of municipal solid wastes." *Waste Manage.*, 29(1), 86–95.

Dixon, N., Langer, U., and Gotteland, P. (2008). "Classification and mechanical behavior relationships for municipal solid waste: Study using synthetic wastes." *J. Geotech. Geoenviron. Eng.*, 134(1), 79–90.

Durmusoglu, E., Sanchez, I. M., and Corapcioglu, M. Y. (2006). "Permeability and compression characteristics of municipal solid waste samples." *Environ. Geol.*, 50(6), 773–786.

Edil, T., Ranguette, V., and Wuellner, W. (1990). "Settlement of municipal refuse." *Geotechnics of waste fills—Theory and practice, STP 1070*, A. O. Landva and G. D. Knowles, eds., ASTM, West Conshohocken, PA, 225–239.

Eleazer, W. E., Odle, W. S., Wang, Y.-S., and Barlaz, M. A. (1997). "Biodegradability of municipal solid waste components in laboratory-scale landfills." *Environ. Sci. Technol.*, 31(3), 911–917.

El-Fadel, M., and Khoury, R. (2000). "Modeling settlement in MSW landfills: A critical review." *Crit. Rev. Environ. Sci. Technol.*, 30(3), 327–361.

Gabr, M. A., and Valero, S. N. (1995). "Geotechnical properties of municipal solid waste." *Geotech. Test. J.*, 18(2), 241–251.

Gourc, J. P., Staub, M. J., and Conte, M. (2010). "Decoupling MSW settlement into mechanical and biochemical processes—modeling and validation on large-scale setups." *Waste Manage.*, 30(8-9), 1556–1568.

Handy, R. L. (2002). "First-order rate equations in geotechnical engineering." *J. Geotech. Geoenviron. Eng.*, 128(5), 416–425.

Hanson, J. L., Yesiller, N., Von Stockhausen, S. A., and Wong, W. W. (2010). "Compaction characteristics of municipal solid waste." *J. Geotech. Geoenviron. Eng.*, 136(8), 1095–1102.

Holtz, R. D., and Kovacs, W. D. (1981). *An introduction to geotechnical engineering*, Prentice-Hall, Upper Saddle River, NJ.

Hossain, M. S., and Gabr, M. A. (2009). "The effect of shredding and test apparatus size on compressibility and strength parameters of degraded municipal solid waste." *Waste Manage.*, 29(9), 2417–2424.

Hossain, M. S., Gabr, M. A., and Barlaz, M. A. (2003). "Relationship of compressibility parameters to municipal solid waste decomposition." *J. Geotech. Geoenviron. Eng.*, 129(12), 1151–1158.

Hull, R. M., Krogmann, U., and Strom, P. F. (2005). "Composition and characteristics of excavation materials from a New Jersey landfill." *J. Environ. Eng.*, 131(3), 478–490.

Jessberger, H. L., and Kockel, R. (1995). "Determination and assessment of the mechanical properties of waste materials." *Geotechnics related to the environment*, R. W. Sarsby, ed., Balkema, Rotterdam, Netherlands, 313–322.

Kavazanjian, E., Jr., Matasovic, N., and Bachus, R. C. (1999). "Large-diameter static and cyclic laboratory testing of municipal solid waste." *Proc., 7th Int. Waste Management and Landfill Symp.*, CISA, Environmental Sanitary Engineering Centre, Cagliari, Italy, 437–444.

Landva, A. O., Valsangkar, A. J., and Pelkey, S. G. (2000). "Lateral earth pressure at rest and compressibility of municipal solid waste." *Can. Geotech. J.*, 37(6), 1157–1165.

Marques, A. C. M., Filz, G. M., and Vilar, O. M. (2003). "Composite compressibility model for municipal solid waste." *J. Geotech. Geoenviron. Eng.*, 129(4), 372–378.

McDougall, J. (2007). "A hydro-bio-mechanical model for settlement and other behaviour in landfilled waste." *Comput. Geotech.*, 34(4), 229–246.

McDougall, J. R., Pyrah, I. C., Yuen, S. T. S., Monteiro, V. E. D., Melo, M. C., and Juca, J. F. T. (2004). "Decomposition and settlement in landfilled waste and other soil-like materials." *Geotechnique*, 54(9), 605–609.

Ng, A. M. Y., Yeung, A. T., Lee, P. K. K., and Tham, L. G. (2006). "Design, fabrication, and assembly of a large oedometer." *Geotech. Test. J.*, 29(4), 298–305.

Olivier, F., and Gourc, J. P. (2007). "Hydro-mechanical behavior of municipal solid waste subject to leachate recirculation in a large-scale compression reactor cell." *Waste Manage.*, 27(1), 44–58.

Olivier, F., Gourc, J. P., Lopez, S., Benhamida, S., and Van Wyck, D. (2003). "Mechanical behavior of solid waste in a fully instrumented prototype compression box." *Proc., 9th Int. Waste Management and Landfill Symp.*, CISA, Environmental Sanitary Engineering Centre, Cagliari, Italy, 1–12.

Oweis, I. S., and Khera, R. P. (1990). *Geotechnology of waste management*, Butterworth, London.

Owens, J. M., and Chynoweth, D. P. (1993). "Biochemical methane potential of municipal solid waste (MSW) components." *Water Sci. Technol.*, 27(2), 1–14.

Rao, S. K., Moulton, L. K., and Seals, R. K. (1977). "Settlement of refuse landfills." *Proc., Conf. on Geotechnical Practice for Disposal of Solid Waste Materials*, Ann Arbor, MI, ASCE, New York, 574–598.

Reddy, K. R., Gangathulasi, J., Parakalla, N. S., Hettiarachchi, H., Bogner, J., and Lagier, T. (2009a). "Compressibility and shear strength of municipal solid waste under short-term leachate recirculation operations." *Waste Manage. Res.*, 27(6), 578–587.

Reddy, K. R., Hettiarachchi, H., Gangathulasi, J., Bogner, J. E., and Lagier, T. (2009b). "Geotechnical properties of synthetic municipal solid waste." *Int. J. Geotech. Eng.*, 3(3), 429–438.

Reddy, K. R., Hettiarachchi, H., Parakalla, N. S., Gangathulasi, J., and Bogner, J. E. (2009c). "Geotechnical properties of fresh municipal solid waste at Orchard Hills landfill, USA." *Waste Manage.*, 29(2), 952–959.

Sivakumar Babu, G. L., Reddy, K. R., Chouskey, S. K., and Kulkarni, H. S. (2010). "Prediction of long-term municipal solid waste landfill

settlement using constitutive model." *Pract. Period. Hazard. Toxic Radioact. Waste Manage.*, 14(2), 139–150.
Sowers, G. (1973). "Settlement of waste disposal fills." *Proc., 8th Int. Conf. on Soil Mechanics and Foundation Engineering*, Vol. 22, Balkema, Rotterdam, Netherlands, 207–210.
Staley, B. F., and Barlaz, M. A. (2009). "Composition of municipal solid waste in the U.S. and implications for carbon sequestration and methane yield." *J. Environ. Eng.*, 135(10), 901–909.
Stoltz, G., and Gourc, J. P. (2007). "Influence of compressibility of domestic waste on fluid permeability." *Proc., Sardinia 11th Int. Waste Management and Landfill Symp.*, CISA, Environmental Sanitary Engineering Centre, Cagliari, Italy, 1–8.
Stoltz, G., Gourc, J. P., and Oxarango, L. (2010). "Characterization of the physic-mechanical parameters of MSW." *Waste Manage.*, 30(8-9), 1439–1449.
Terzaghi, K., Peck, R. B., and Mesri, G. (1996). *Soil mechanics in engineering practice*, 3rd Ed., Wiley, New York.
Vilar, O. M., and Carvalho, M. F. (2004). "Mechanical properties of municipal solid waste." *J. Test. Eval.*, 32(6), 438–449.
Zekkos, D., et al. (2006). "Unit weight of municipal solid waste." *J. Geotech. Geoenviron. Eng.*, 132(10), 1250–1261.

Copyright of Journal of Geotechnical & Geoenvironmental Engineering is the property of American Society of Civil Engineers and its content may not be copied or emailed to multiple sites or posted to a listserv without the copyright holder's express written permission. However, users may print, download, or email articles for individual use.